



ELSEVIER

Available online at www.sciencedirect.com

ScienceDirect

journal homepage: www.elsevier.com/locate/ijhydene

Full Length Article

Design and implementation of a new contactless triple piezoelectrics wind energy harvester

Erol Kurt ^a, Francesco Cottone ^b, Yunus Uzun ^{c,*}, Francesco Orfei ^b,
Maurizio Mattarelli ^b, Davut Özhan ^d^a Department of Electrical and Electronics Engineering, Gazi University, TR-06500, Teknikokullar, Ankara, Turkey^b Department of Physics and Geology, University of Perugia, 06123, Perugia, Italy^c Department of Electrical and Electronics Engineering, Aksaray University, Aksaray, Turkey^d Mardin Vocational School, Artuklu University, Mardin, Turkey

ARTICLE INFO

Article history:

Received 16 November 2016

Received in revised form

29 January 2017

Accepted 23 February 2017

Available online xxx

Keywords:

Piezoelectric

Triple

Contactless

Wind energy

Harvester

Power

ABSTRACT

The features of the new designed and constructed harvester are examined. The harvested power of three piezoelectric layers having different masses (i.e. different natural frequencies) has been explored. These layers have the same length around the harvester body, whereas a permanent magnet (PM) attached to the shaft rotates by low speed wind and this PM repels these three piezoelectric layers with a 120° phase shift. Since PM and the PMs located to the tip of the layers do not contact, this system improves the lifetime of the harvester. The measured harvested power in the low wind speeds (i.e. 1.75 m/s) is of the order of 0.2 μ W. The waveform includes many subharmonic and superharmonic components, hence the total harmonic distortion (THD) is found around 130%, which is fairly high due to nonlinear effects. Although the system shows an high THD, the 20% of the signal can be rectified and stored in the capacitor for the use of harvested energy. A scenario has also been created for a resistive load of $R_L = 1\text{ M}\Omega$ and 100 k Ω for various wind speeds and it has been proven that the harvester can feed the load at even lower wind speeds. In addition, extra power beyond the usage of the load can be stored into the capacitor. The proposed harvester and its rectifying unit can be a good solution for the energy conversion procedures of low-power required machines.

© 2017 Hydrogen Energy Publications LLC. Published by Elsevier Ltd. All rights reserved.

Introduction

There exist growing works on the long-life energy required devices such as unmanned aerial vehicles, sensor nodes, pacemakers, etc [1–3]. After the recent improvements in

nanotechnology, many piezoelectric materials and related structures can be fabricated from micro to macro-scales in various geometries upon the application needed [4,5]. In that frame, macrostructures or devices such as bicycles, shoes, arm and leg connected piezo-powered systems have also been frequently studied in addition to micro structures [6–9].

* Corresponding author. Fax: +90 312 2028550.

E-mail address: yunusuzun38@hotmail.com (Y. Uzun).

<http://dx.doi.org/10.1016/j.ijhydene.2017.02.157>

0360-3199/© 2017 Hydrogen Energy Publications LLC. Published by Elsevier Ltd. All rights reserved.

Nowadays, the literature has many harvester applications [10]. As the main goal to generate energy, leaf type piezoelectric generators [11], contacted windmills [12,13], two degrees of freedom beam type wind generators [14] and flow induced self excited wind power generators [15] can be mentioned. Many of them are operated with mechanically contacting piezoelectric layers [16].

As the most compact harvester tool, piezoelectric materials are widely used for the wireless devices in nature, industry and human activities [17–20]. It is mainly due to their easy installation and maintenance, compact structure and high energy density [21]. According to last technological achievements, it has become much cheaper relative to the past years. For that reason, piezoelectric components start to find good place among the other energy conversion systems such as solar panels, thermoelectric generators, etc.

By considering the low energy requirements, the piezoelectric generators give a power scale of μW or mW , which are already sufficient for many engineering applications. On the one hand, most of the electrical devices use batteries and that creates the maintenance problems because of the either the environmental issues or their complex recycling processes. Besides, the lifetime of a battery is too limited and this lifetime can be increased further by different external and environmental-friendly resources [22,23]. In that context, an additional piezoelectric harvester can be mounted to charge the batteries in real time or feed the device itself, continuously.

The harvesters are such devices that can convert ambient vibrations into a useful electrical energy. The main research activity aiming at improving the harvesting performance is into three main groups: the production of piezoelectric materials, the design of mechanical systems and the implementation of efficient conversion circuit. Although the harvested energy per material volume of a piezoelectric is higher than any conventional solar and wind energy applications, piezo-systems have some issues and should be further improved for better energy solutions. For instance, the wind speeds of our interest are in the range of 1.6 m/s – 3.2 m/s due to the fact that the generated force from small blades (around 1.3×10^{-3} – $3.2 \times 10^{-3} \text{ m}^2$) is too small around 0.1 N at those speeds. That condition makes the use of any type of electromagnetic harvester or conventional turbines be impossible, thereby the piezoelectric-based devices have certain advantages for the feeding of small-scale devices in that manner. However, the other task should be the solution to the artifacts stated above by designing those.

The main objective of the present study is to show the useful electrical power generation from the present complicated voltage waveforms and characterize the output power with a resistive load for various wind speeds. In addition, this new harvester with triple piezoelectric layers is introduced for a micro-range power generation without any mechanical contact. Therefore it has certain advantages to increase the mechanical durability of the system and piezoelectrics as well. The proposed harvester can be used in low power applications being far away from any electrical grid and it can be fed at low wind speeds and an extension to the life-span of the battery can be enabled. Besides, the energy range can be increased further by using thicker piezoelectric layers in the same harvester.

The paper is organized as follows: Section **The experimental setup of the harvester** gives some introductory information on the design and construction of new harvester and the preliminary tests. Section **Theoretical background** provides a brief explanation of the theory as the preparation to the time-dependent simulations. Experimental results carried out in wind tunnel along with power consumption features of the weather station are presented in Section **Results and Discussion**. Finally, the concluding remarks are given in the **Conclusions Section**.

The experimental setup of the harvester

The wind energy harvester consists of four main parts (see in Fig. 1(a)): A propeller which can rotate freely by the wind, a shaft transferring the mechanical rotation to the magnet, a piezoelectric unit including three layers and the electronic part, which is responsible to regulate and store the harvested electrical signal from the terminals of the piezoelectric layers.

The three layer structure of the harvester occurs due to three separate piezoelectric layers, which are located with 120° angle to each other on a circular geometry. Each layer tip having a small permanent magnet is oriented in such a way that the magnet on the shaft can repel it when it comes to the opposite. Although the device has three identical piezoelectric layers, the magnet numbers at the tip of them differs. Indeed, that affects the natural frequency of the layers due to the increase at the magnet mass. The higher mass creates lower frequency due to the buckling formation along the gravity. Note that in order to provide the security of the layers, a cylindrical polyethylene material has been fixed on the shaft. It prevents the damage of the piezoelectric layers especially at high wind speeds, since the nonlinear effects can attract the layers into the shaft and that lead to damages on the layer. When the wind flows through the blades as in the wind tunnel tests (see in Fig. 1(b)), the shaft rotates about the shaft axis and the permanent magnet attached to the middle of the shaft just inside the polyethylene material is rotated. A more detailed form of the setup is presented in Fig. 1(c and d) in order to determine the units of harvester and its operational parts. The blades are directly connected to the central shaft, which is responsible to transfer the rotational movement to the permanent magnet housed in the polyethylene cylinder at the right side (Fig. 1(d)). Note that the cylinder has certain lateral regions in order to stop the tip of the layers, thereby prevent them to be damaged. As shown in Fig. 1(c), the body part of the harvester includes all the piezoelectrics, which are responsible to generate electricity from the mechanical oscillations. When the magnet gets closer to each layer tip, the layer has been bent without any mechanic contact, since the poles of the magnets have been adjusted same. Every wind speed creates a vibration and that is then transferred into the electrical potential on the layers.

This wind energy harvester has a novel structure due to its contactless operation to the shaft. According to the literature, we have another contactless harvester study, however it is a single layer device and has much harmonics [24]. Indeed, the optimal power generation is an important task for such systems, which has high harmonic waveforms. Within that

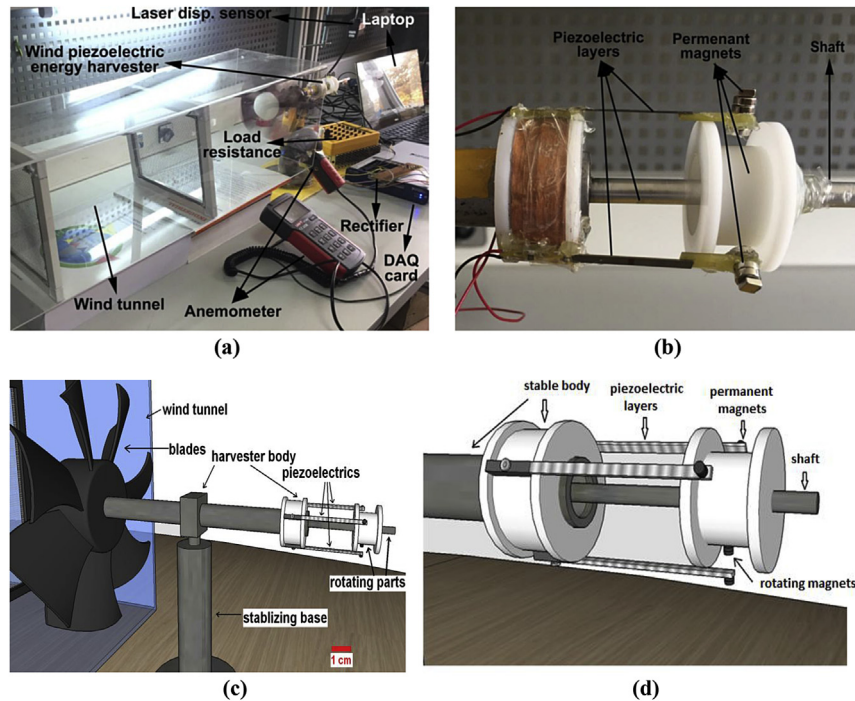


Fig. 1 – (a) The proposed wind energy harvester and test setup, (b) piezoelectric layers and magnets. (c) The sketch of the harvester with size. (d) The closed view of rotating components.

study, we offer a suitable rectifier and storage circuit by applying two different cases for different electrical resistive loads R_L . Each piezoelectric layer has the dimensions of $41.3 \text{ mm} \times 4.7 \text{ mm} \times 1.5 \text{ mm}$ and the weight of 1.1 g . Besides, its capacitance and stiffness values are 12 nF and 61 N/m , respectively. In the experiments, a data acquisition system with NI USB-6250 DAQ has been used. This card has 16 analog inputs and it can make multiple records of displacement and harvested voltages, synchronously.

The experimental setup is shown in Fig. 1(a). The harvester operates in the wind tunnel tests. The experimental setup includes an anemometer measuring the wind speed of the tunnel. During these tests, wind speeds have been adjusted between $v = 1.6 \text{ m/s}$ to 3.2 m/s , which are fairly less than the speeds for the conventional wind generators. The setup also includes a laser displacement sensor, a laptop for data recordings and resistive loads. Fig. 1(b) shows the detail of the layers and the magnets.

In Fig. 2, the schematic representation of the rectifier-storage circuit is given. The waveforms from the terminals of three piezoelectric layers are given to the input of a three

phase full bridge rectifier. Here BAS70 type diodes with low Schottky barriers have been used for the best performance. From the output of the rectifier the rectified waveform has been given to the capacitor C1 of capacitance equal to $100 \mu\text{F}$. Note also that different resistive loads have also been attached at the output of the circuit in order to observe the performance of the harvester. In the schematic of Fig. 2 a $100 \text{ k}\Omega$ resistor has been placed after the rectifier to evaluate the performance of the generators under load condition.

The simulations have been carried on using a SPICE simulator from Texas Instruments, TINA TI. As it can be seen in Fig. 2, three voltage generators have been placed in the simulator to represent each of the three piezoelectric harvesters. The model of the generator used in the simulator corresponds to an arbitrary generator: it requires a definition of the voltage waveform (a time series in WAV format), its peak amplitude and the internal impedance.

The WAV time series and the peak amplitudes have been obtained from real measurements of the harvesters with an oscilloscope.

The maximum power extraction for a piezoelectric generator is achieved at the working point located at one half of open circuit voltage V_{oc} with a corresponding current equal to one half of its closed circuit current I_{cc} . Taking into account these considerations, the internal impedance of the piezoelectric energy harvester which is equal to the optimal load can be obtained from the datasheet parameters [25,26] of the piezoelectric element (Piezo Systems model D220-A4-503YB) as follows.

$$R_{opt} = \frac{V_{oc}}{I_{cc}} \approx 8.5 \text{ k}\Omega \leftrightarrow P_{max} = \frac{1}{4} \frac{V_{oc}^2}{R_{opt}}$$

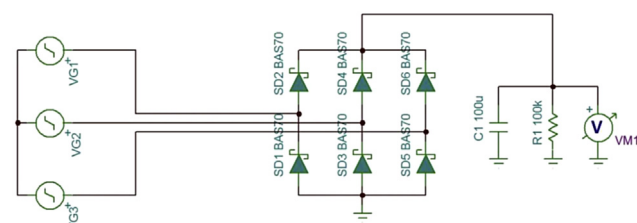


Fig. 2 – Three phase full bridge rectifier and storage circuit.

Given this value, the results of the simulation are presented in Fig. 3. Since the piezoelectrics indicate mostly a capacitive media due to its dielectric properties, Fig. 3 provides a good solution on the energy storage feature of three piezoelectrics. Note that the circuit in Fig. 2 is used to rectify the waveforms in order to charge the capacitor.

As it can be seen, even with a 100 kΩ load connected to the rectifier, the voltage across the capacitor reaches a value close to 22 V in about 8 s. This is well visible in Fig. 4. Moreover, from the same plot is possible to note how the three generators produce different voltages rich of harmonics. This is mainly due to different resonance frequencies of the three energy harvesters.

Fig. 5 has been measured directly from the terminals of three piezoelectric layers via an oscilloscope. Before the rectifier has rectified the waveforms, all waveforms are seen to be highly distorted.

Due to harmonics and distortions, an ordinary three phase formation cannot be obtained, clearly for this new harvester. The three harvesters have different behavior since the masses placed on the tip are different and can be adjusted via adding a different number of permanent magnets: That yields to different natural frequencies and waveforms as a result.

Theoretical background

The theoretical expression of the proposed harvester can be stated as follows:

$$\frac{d\theta}{dt} = \omega, \quad (1)$$

$$m_1 \frac{d^2 r_1}{dt^2} = -kr_1 - \gamma \frac{dr_1}{dt} + \alpha v_1 + f_m \delta(\theta - \theta_1), \quad (2)$$

$$m_2 \frac{d^2 r_2}{dt^2} = -kr_2 - \gamma \frac{dr_2}{dt} + \alpha v_2 + f_m \delta(\theta - \theta_2), \quad (3)$$

$$m_3 \frac{d^2 r_3}{dt^2} = -kr_3 - \gamma \frac{dr_3}{dt} + \alpha v_3 + f_m \delta(\theta - \theta_3), \quad (4)$$

$$I_1 = \alpha \frac{dr_1}{dt} - C \frac{dv_1}{dt}, \quad (5)$$

$$I_2 = \alpha \frac{dr_2}{dt} - C \frac{dv_2}{dt}, \quad (6)$$

$$I_3 = \alpha \frac{dr_3}{dt} - C \frac{dv_3}{dt}, \quad (7)$$

where, θ , ω , δ , m , r , u , α , V , f_m , θ_A , C , I and k indicate angular position of the magnet, propeller speed, Kronecker delta which gives “1” for $\theta = \theta_i$ ($i = 1 \dots 3$) else “0”, mass of the layer, radial position to center of shaft, mass displacement of layer, force factor of layer, voltage between the layer terminals, magnetic force of magnet, angular position of layer, layer capacitance, harvested current and stiffness constant of the layer, respectively. For a similar formulation of a different system, we refer to our earlier studies [27,28].

In order to obtain the dimensionless form, we introduce a time constant $\tau = \omega_0 t$ into the derivatives in Eqs. (1)–(7). One arrives at the following for the dimensionless equations:

$$\frac{d\theta}{d\tau} = \frac{\omega}{\omega_0}, \quad (8)$$

$$\frac{d^2 r_1}{d\tau^2} = -r_1 \left(1 + \frac{f_{11} \text{Sin}(\theta) \delta(\theta - \theta_1)}{k} \right) - \Gamma_1 \frac{dr_1}{d\tau} - A_1 v_1 + F_{01} \text{Sin}(\theta) \delta(\theta - \theta_1), \quad (9)$$

$$\frac{d^2 r_2}{d\tau^2} = -r_2 \left(\frac{m_1}{m_2} + \frac{m_1 f_{12} \text{Sin}(\theta) \delta(\theta - \theta_2)}{k} \right) - \Gamma_2 \frac{dr_2}{d\tau} - A_2 v_2 + F_{02} \text{Sin}(\theta) \delta(\theta - \theta_2), \quad (10)$$

$$\frac{d^2 r_3}{d\tau^2} = -r_3 \left(\frac{m_1}{m_3} + \frac{m_1 f_{13} \text{Sin}(\theta) \delta(\theta - \theta_3)}{k} \right) - \Gamma_3 \frac{dr_3}{d\tau} - A_3 v_3 + F_{03} \text{Sin}(\theta) \delta(\theta - \theta_3), \quad (11)$$

$$I_1 = \alpha \omega_0 \frac{dr_1}{d\tau} - C \omega_0 \frac{dv_1}{d\tau}, \quad (12)$$

$$I_2 = \alpha \omega_0 \frac{dr_2}{d\tau} - C \omega_0 \frac{dv_2}{d\tau}, \quad (13)$$

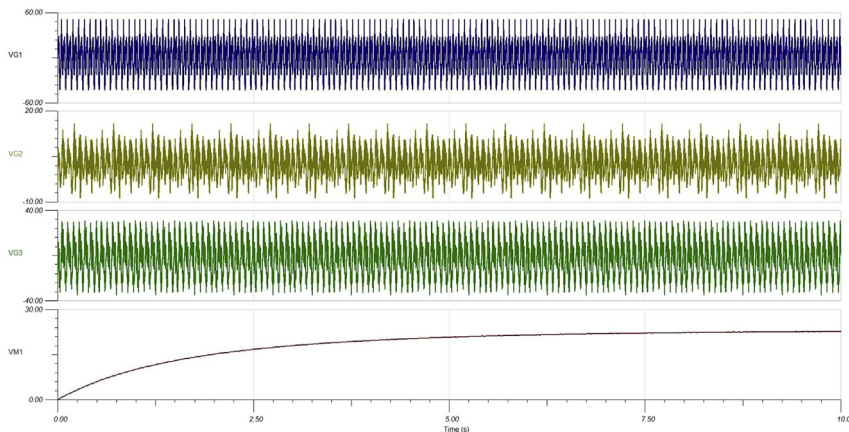


Fig. 3 – Simulation of the charging of a 100 μF capacitor with the three piezoelectric energy harvesters.

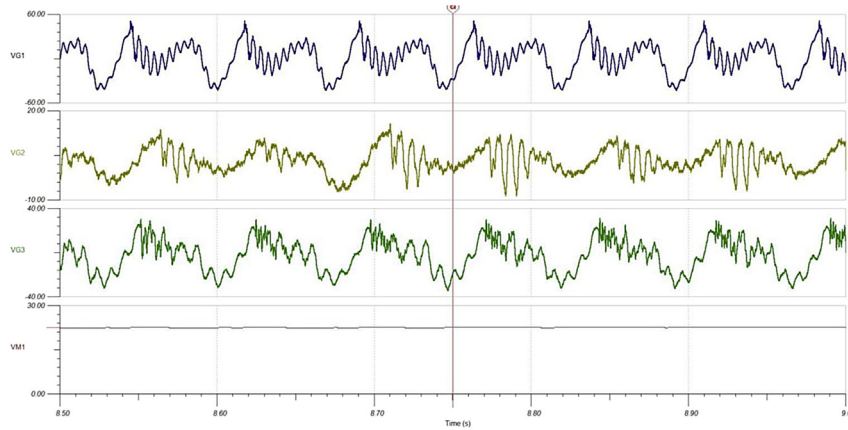


Fig. 4 – Detail of the simulation of the charging of a 100 μF capacitor with the three piezoelectric energy harvesters: the voltage at the position of the marker “a” is equal to 22.4 V.

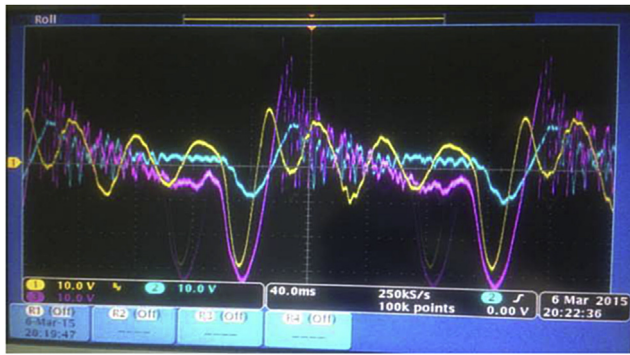


Fig. 5 – Oscilloscope view of the waveforms of three piezoelectric layers for $R_L = 800 \text{ k}\Omega$. The wind speed is 3.2 m/s.

$$I_3 = \alpha\omega_0 \frac{dr_3}{d\tau} - C\omega_0 \frac{dv_3}{d\tau}, \quad (14)$$

where $f_{mi} = \sin(\theta) (f_{0i} + (d - r_i) f_{1i})$ is considered according to our previous studies under the magnetic field, which has a rotation effect [28,29] Here i denotes the piezoelectric index as before.

Since the magnetic force is a displacement-dependent function, the expression should include at least the linear dependence to the position r . Since the higher order terms of the magnetic force f_m is out of the scope of the present study, we do not consider it for now. However, if d as the distance from the tip of the piezoelectric to the magnet located on the shaft is closed, more contribution will be from f_0 and f_1 in that regard.

The systems parameters can be stated as follows after the dimensionless forms:

(a) The magnetic force strengths:

$$F_{01} = \left(\frac{f_0 + d f_1}{k} \right), \quad (15)$$

$$F_{02} = \left(\frac{f_{02} + d f_{12}}{m_2 \omega_0^2} \right), \quad (16)$$

$$F_{03} = \left(\frac{f_{03} + d f_{13}}{m_3 \omega_0^2} \right), \quad (17)$$

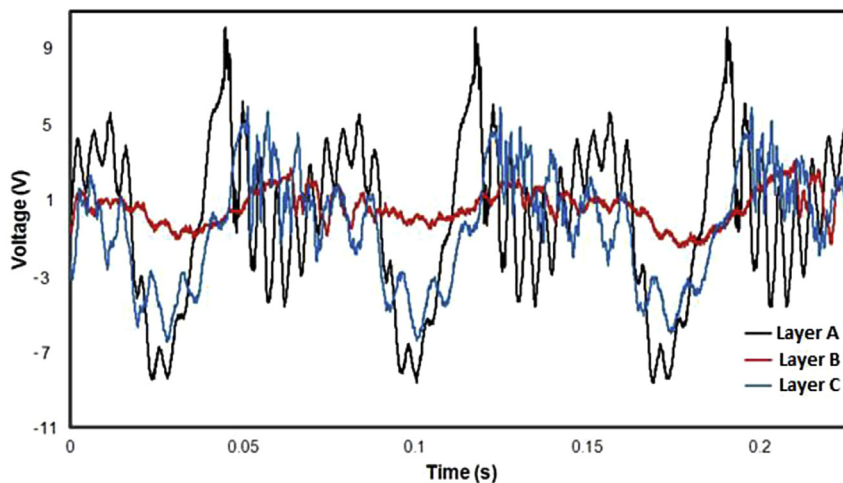


Fig. 6 – Three representative waveforms from three layers at the wind speed $v = 2.88 \text{ m/s}$.

(b) The damping coefficients:

$$\Gamma_1 = \frac{\gamma}{k} \quad (18)$$

$$\Gamma_2 = \frac{\gamma}{m_2 \omega_0} \quad (19)$$

$$\Gamma_3 = \frac{\gamma}{m_3 \omega_0} \quad (20)$$

(c) Force factors:

$$A_1 = \frac{\alpha}{k} \quad (21)$$

$$A_2 = \frac{\alpha m_1}{m_2 k} \quad (22)$$

$$A_3 = \frac{\alpha m_1}{m_3 k} \quad (23)$$

(d) The natural angular frequency of a piezoelectric:

$$\omega_0 = \sqrt{\frac{k}{m_1}} \quad (24)$$

By considering the equations above, a numerical approach can be used to determine the tip position, velocity, generated current and voltage by using a Runge–Kutta time integration in MatLab. For this aim, we should transform the second order differentiations to first order forms. If we denote the tip velocity of the piezoelectrics with u , one arrives at the following:

$$\frac{d\theta}{d\tau} = \frac{\omega}{\omega_0}, \quad (25)$$

$$\frac{dr_1}{d\tau} = u_1 \quad (26)$$

$$\frac{du_1}{d\tau} = -r_1 \left(1 + \frac{f_{11} \text{Sin}(\theta) \delta(\theta - \theta_1)}{k} \right) - \Gamma_1 u_1 - A_1 v_1 + F_{01} \text{Sin}(\theta) \delta(\theta - \theta_1), \quad (27)$$

$$\frac{dr_2}{d\tau} = u_2 \quad (28)$$

$$\frac{du_2}{d\tau} = -r_2 \left(\frac{m_1}{m_2} + \frac{m_1 f_{12} \text{Sin}(\theta) \delta(\theta - \theta_2)}{k} \right) - \Gamma_2 u_2 - A_2 v_2 + F_{02} \text{Sin}(\theta) \delta(\theta - \theta_2), \quad (29)$$

$$\frac{dr_3}{d\tau} = u_3 \quad (30)$$

$$\frac{du_3}{d\tau} = -r_3 \left(\frac{m_1}{m_3} + \frac{m_1 f_{13} \text{Sin}(\theta) \delta(\theta - \theta_3)}{k} \right) - \Gamma_3 u_3 - A_3 v_3 + F_{03} \text{Sin}(\theta) \delta(\theta - \theta_3), \quad (31)$$

$$I_1 = \alpha \omega_0 \frac{dr_1}{d\tau} - C \omega_0 \frac{dv_1}{d\tau}, \quad (32)$$

$$I_2 = \alpha \omega_0 \frac{dr_2}{d\tau} - C \omega_0 \frac{dv_2}{d\tau}, \quad (33)$$

$$I_3 = \alpha \omega_0 \frac{dr_3}{d\tau} - C \omega_0 \frac{dv_3}{d\tau}, \quad (34)$$

The currents I can be determined by v/R_L as usual, when the electrical load is connected to each piezoelectrics. Note that v denotes the harvested voltages as defined before. A representative simulation result will be given in the next section by introducing them into the MatLab as the first order differential equations. Here the wind speed is introduced as the angular velocity ω to the equations.

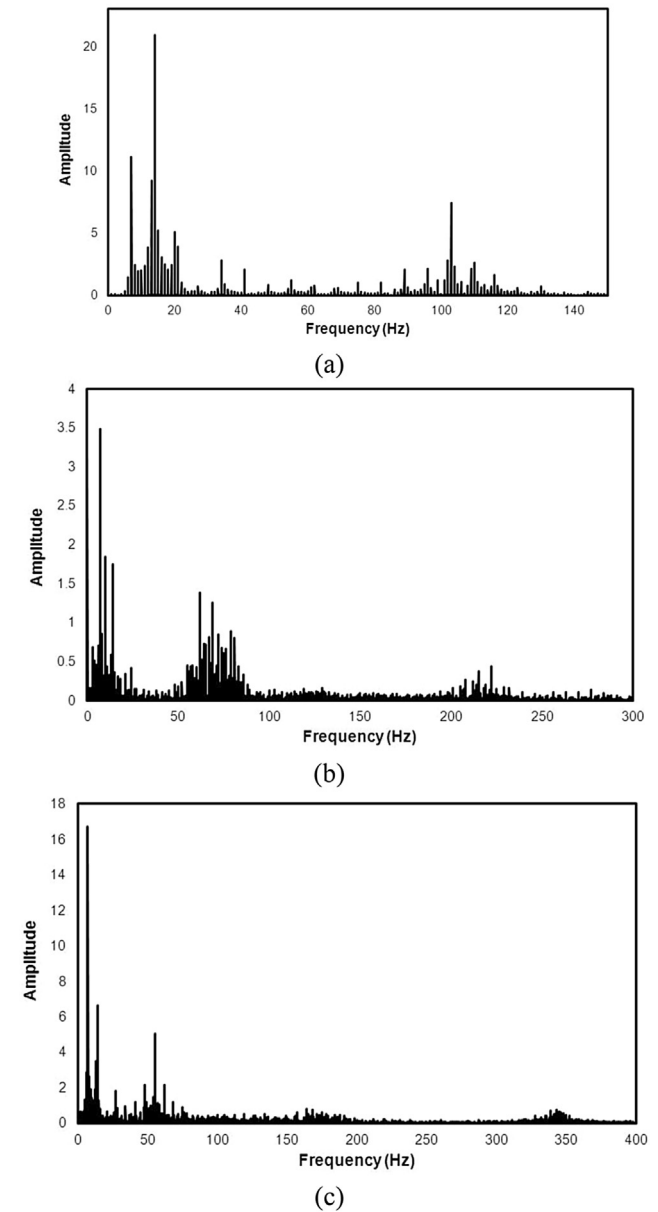


Fig. 7 – FFT results of the waveforms in Fig. 6: (a) Layer A, (b) Layer B and (c) Layer C.

According to this formulation, when the propeller rotates with an angular velocity ω , that mechanical effect is transmitted to the radial position r for the corresponding layer, which are denoted by 1, 2 and 3 indice. Note that different tip masses m_1 , m_2 and m_3 affect the natural frequencies of the buckling layers, hence modifying the generated waveform. When the radial distance changes via the buckling, the piezoelectric layers generate currents at their terminals, which are defined by Eqs. (32)–(34). Note that the electrical current depends on the velocity and the potential change by time. While the potential changes, the charge amount is changed inside the piezo-material [30].

Results and discussion

After the construction of the setup in Fig. 1(a), we tested the energy harvesting mechanism and the rectifying and storing circuit at different wind speeds in the wind tunnel. Initially we acquired the natural waveforms directly from the terminals of the layers. The voltages of three piezoelectric layers are given in Fig. 6. Each layer has been shown in different colors (in the web version). The signal amplitudes can change due to different tip masses of the harvester. This data were recorded at the wind speed $v = 2.88$ m/s. The system can produce voltages up to 12 V depending on the wind speed.

According to these waveforms, the system produces high degrees of harmonics which makes the rectification process a complicated task. Here, we aim at exploring and implementing an efficient rectifying circuit. Therefore, we first analyzed

the FFT of the waveforms of each layer. The FFT analysis results are presented in Fig. 7(a–c).

The results prove that each layer has different frequency combination. While Layer A has maximal frequencies up to 130 Hz, Layer B has 280 Hz and the last layer has 350 Hz. The main frequencies of all layers have various values. Strictly speaking, they are $f = 13$ Hz, $f = 7$ Hz and 5 Hz for Layers A, B and C, respectively. Note that there are some frequency clusters for each of them. A detailed analysis on the waveform of Layer A proves that 7 Hz, 105 Hz, 20 Hz, 35 Hz, 90 Hz, 98 Hz and 42 Hz are key components of the frequency spectrum (Fig. 7(b)). In the case of Layer B, the leading components can be counted as 9 Hz, 13 Hz, 60 Hz, 66 Hz and 78 Hz. The last layer has the leading components of 10 Hz, 53 Hz, 49 Hz and 58 Hz (Fig. 7(c)). The high frequency components have the lowest amplitudes and they do not contribute significantly to the power generation from these waveforms. In terms of harmonics analysis, we have also conducted a detailed analysis on the total harmonic distortions (THDs). While the THD value of Layer A is found as 101%, the THD values of Layer B and C are found as 132% and 70%, respectively. As also clarified from those values, the waveforms are highly distorted.

As the most important experimental exploration, we have applied two variable wind speed regimes as in Fig. 8(a and b) in order to test the new harvesting system in conditions similar to the natural environment. In Fig. 8(a), the electrical load $R_L = 1$ M Ω is used for the power extraction from the system. The wind tunnel has started to rotate the propeller of the harvester with $v = 2.23$ m/s as in Fig. 8(a). At lower speed than 1.75 m/s, the capacitor does not store sufficient charges,

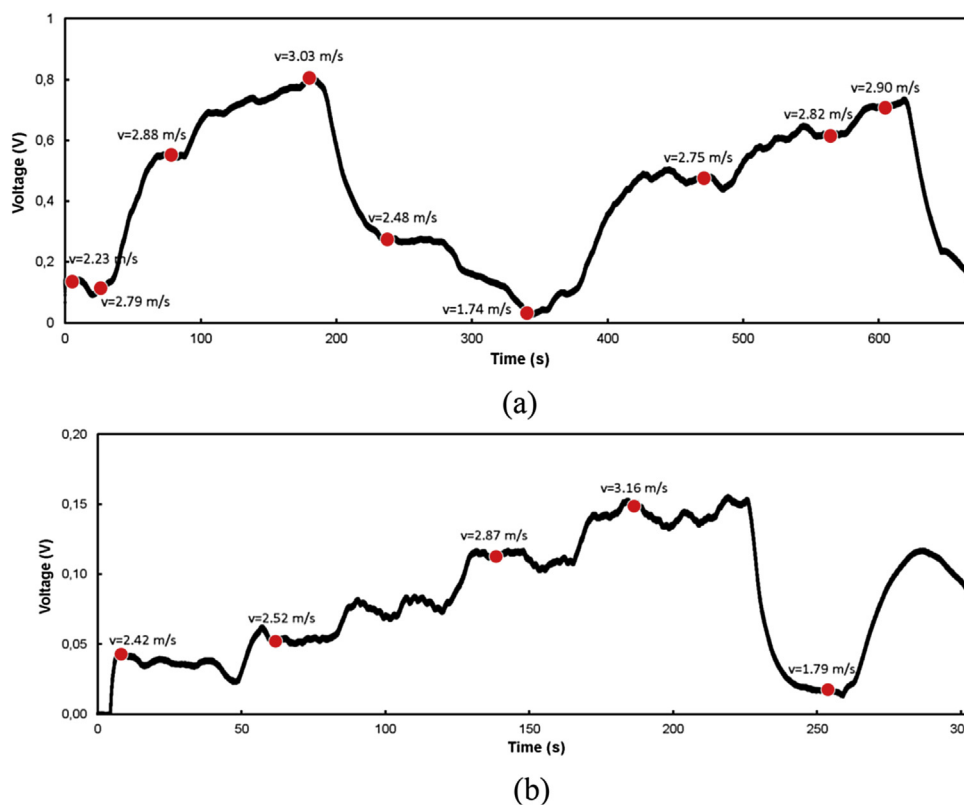


Fig. 8 – Wind tunnel tests under random wind speeds. (a) Resistive load is $R_L = 1$ M Ω and (b) $R_L = 100$ k Ω .

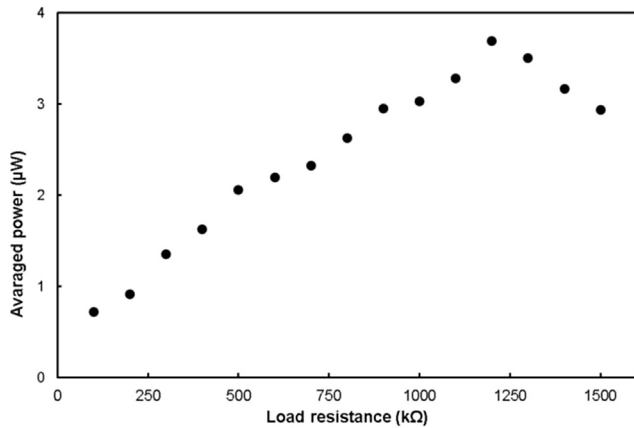


Fig. 9 – The total harvested power from the terminals of piezoelectric layers at 3.03 m/s.

therefore the voltage generated is directly spent on the load. However, when the wind speed becomes $v = 2.79$ m/s, the voltage across the capacitance (i.e. resistive load at the same time) increases dramatically. Even on the plateau between 70 s and 90 s, the capacitor charges up to nearly 0.6 V. On that plateau, the wind speed gradually increases up to 2.88 m/s and the voltage increases at the storage circuit up to 0.82 V when wind flows with 3.03 m/s. After suddenly decreasing the wind speed down to 2.48 m/s, as encountered in nature, the energy stored is spent into the load between 180 s and 230 s. However, the speed 2.48 m/s is still high enough to produce more energy than the consumed. Another plateau occurs around 0.3 V between 230 m/s and 280 m/s. However, when the wind speed decreases down to $v = 1.74$ m/s, the power stored in the capacitor is about to vanish. This cyclic behavior restarts after 350 s, when another flow with 2.75 m/s speeds up the generator and the voltage increases at 0.5 V. Note that the load dissipated energy during all the time. In real applications, the user systems usually have stand-by condition, which do not

spend much energy from the capacitor. Therefore, the produced energy can be sufficient for many applications even in that wind speed range. For instance, the power value $1 \mu\text{W}$ stands for the stand-by condition under 1 V with the current amount $1 \mu\text{A}$ for many applications.

In Fig. 8(b), another scenario is tested. While the wind regime resembles to the first case, the load is smaller (i.e. $R_L = 100 \text{ k}\Omega$) for the second case. This load value does not match the generator impedance, so that the harvested power is reduced. However, this test is important in order to see the voltage levels, when the load is changed. An overview into Fig. 8(b) proves that the maximal voltage 0.15 V is obtained at $v = 3.16$ m/s between 180 s and 200 s. However, a gradually increasing trend occurs from the beginning to that value. However, also in this case for wind speed higher than 2.4 m/s the harvester can both drive the user system and store excess energy in the capacitor.

The total harvester power is shown in Fig. 9. It has a maximal value of $3.8 \mu\text{W}$ at $1.15 \text{ M}\Omega$. Further optimizations of such a system must be done. In particular, the maximum power point tracking (MPPT) technique can be a useful to improve the efficiency for variable loads.

When the load is adjusted around $200 \text{ k}\Omega$, nearly the quarter of the optimized power can be reached. There exists a nearly linear power increase with the load. All these measurements have been done without the rectifying and storage circuit. Fig. 10 shows the rectified voltage and power with respect to the wind speed.

The results indicate that the system still harvests energy at $v = 1.75$ m/s. When the speed increases, the harvested power increases slowly. When the speed exceeds the value of 2.25 m/s, the power increases rapidly. After 2.85 m/s, the power increase occurs slowly again. All these features can also be seen in peak voltage in Fig. 6.

In order to provide a simulation result for the proposed harvester model, Eqs. (25)–(34) have been solved with a time integration. Since three of the layers have various mass values, their voltages vary as in Fig. 11.

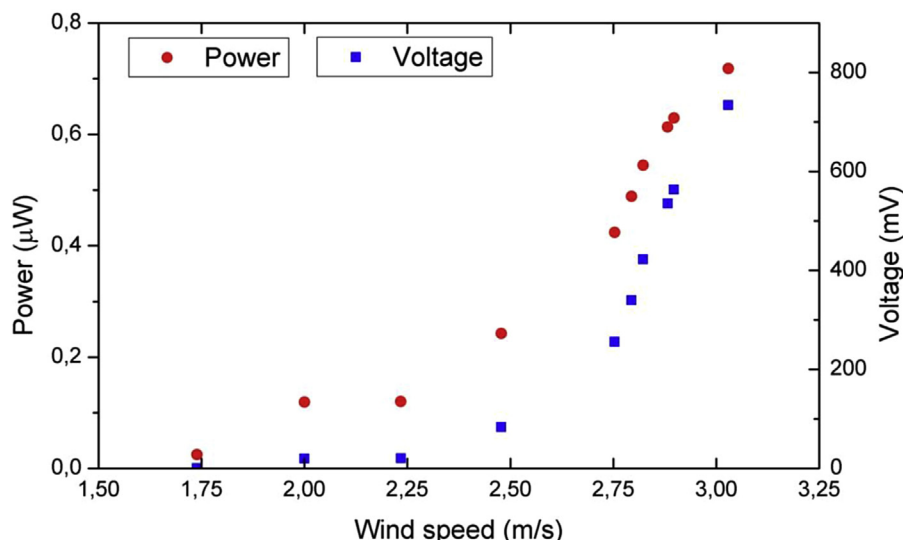


Fig. 10 – The dc voltage and power variation for different wind speeds at $R_L = 1 \text{ M}\Omega$.

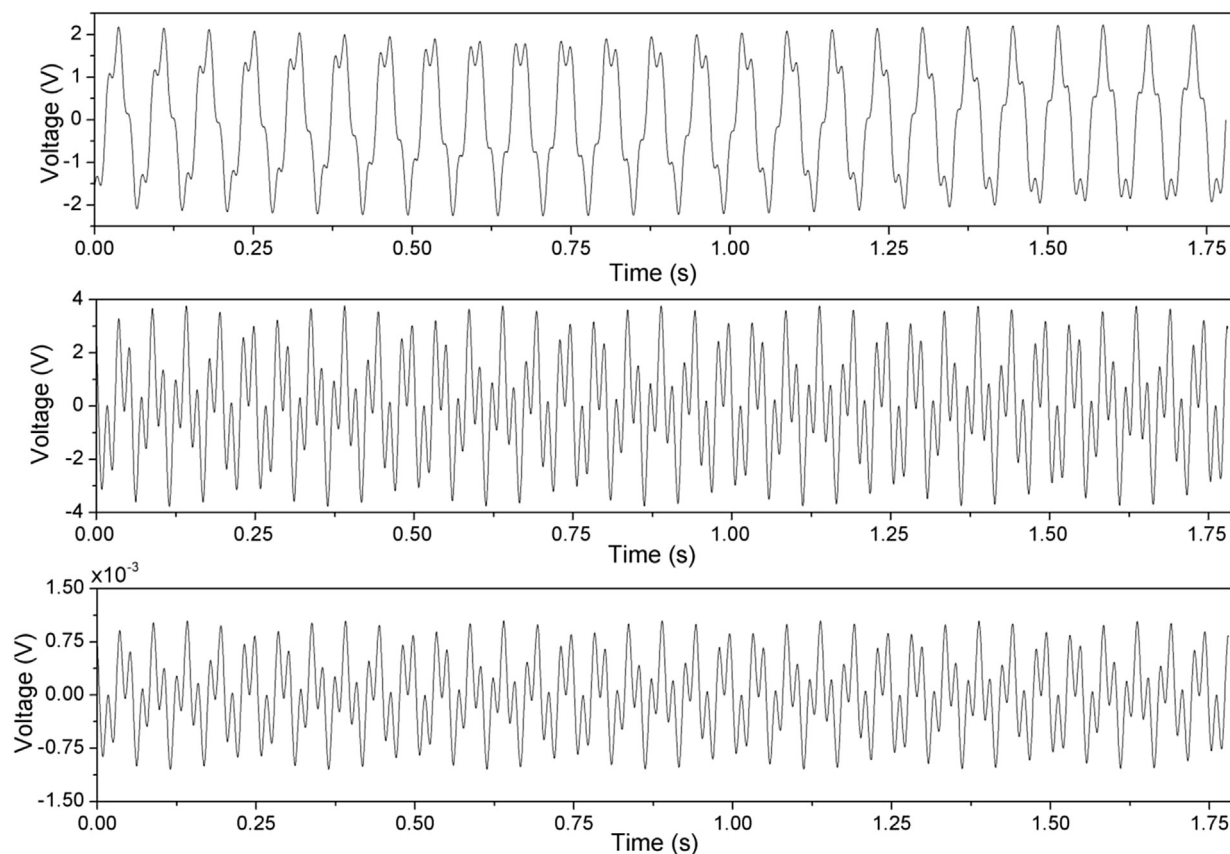


Fig. 11 – The time-dependent simulation results for wind speed 3.1 m/s at $R_L = 100 \text{ k}\Omega$.

Conclusions

The output power characteristics and voltage waveforms of a new type triple piezoelectric layer harvester have been explored. The waveforms from three layers are observed to have different nonlinear features. Although the device has three identical layers, the magnet numbers at the tip of the piezoelectric materials affect the natural frequencies of the layers. The harvested power has been measured as $0.2 \mu\text{W}$ in a low wind speed such as 1.75 m/s. While the power amount from directly piezoelectric terminals has been measured as $3.8 \mu\text{W}$, the nonlinearities in the waveforms prevent to have all of the power as a useful power. The waveforms consist of many subharmonic and superharmonic components, hence the total harmonic distortion (THD) has been found around 130%, which is fairly high due to nonlinear effects. Although the system shows a high THD, the 20% of the signal can be rectified and stored in the capacitor for the use of harvested energy in accordance with the tests. Two scenarios have been created for resistive loads of $R_L = 1 \text{ M}\Omega$ and $100 \text{ k}\Omega$ for variable wind speeds in order to test the performance of the harvester. It has been proven that the harvester feeds the load at even lower wind speeds such as 1.75 m/s. In addition, extra power beyond the usage of the load can be stored into the capacitor for the future usage. The harvester is considered to be a good candidate for the power source of low-power required machines, however an efficient maximum power point tracking

scheme can be used to achieve better solutions for variable electrical loads. In addition, thicker piezoelectrics can be better to increase the harvested energy from the proposed contactless harvester system.

Acknowledgments

This research has been supported by Mardin Artuklu University Scientific Research Unit Council under the Grant No: MAÜ-BAP-16-MYO-19, by The Ministry for European Affairs-National Agency of Turkey under the Grant No: 2015-1-TR01-KA203-021342 (Innovative European Studies on Renewable Energy Systems) and by European Commission under the EU Horizon 2020 Programme Grant Agreement No: 644852, PROTEUS.

REFERENCES

- [1] Hosseinabadi NR, Tabesh A, Dehghani R, Aghili A. An efficient piezoelectric windmill topology for energy harvesting from low-speed air flows. *IEEE Trans Ind Electron* 2015;62:3576–83.
- [2] Erturk A, Renno JM, Inman DJ. Modeling of piezoelectric energy harvesting from an L-shaped beam-mass structure with an application to UAVs. *J Intel Mater Syst Struct* 2009;20:529–44.

- [3] Karami MA, Inman DJ. Powering pacemakers from heartbeat vibrations using linear and nonlinear energy harvesters. *Appl Phys Lett* 2012;100:042901.
- [4] Radousky HB, Liang H. Energy harvesting: an integrated view of materials, devices and applications. *Nanotechnology* 2012;23:502001.
- [5] Harne RL, Wang KW. A review of the recent research on vibration energy harvesting via bistable systems. *Smart Mater Struct* 2013;22:23001.
- [6] Minazara E, Vasic D, Costa F. Piezoelectric generator harvesting bike vibration energy to supply portable devices. In: *Int conf renewable energies and power quality, Santander, Spain*; 2008. p. 1–6.
- [7] Fu H, Xu R, Seto K, Yeatman EM, Kim SG. Energy harvesting from human motion using footstep-induced airflow. *J Phys Conf Ser* 2015;660:012060.
- [8] Pillatsch P, Yeatman EM, Holmes AS. A piezoelectric frequency up-converting energy harvester with rotating proof mass for human body applications. *Sens Actuator A-Phys* 2014;206:178–85.
- [9] Platt SR, Farritor S, Haider H. On low-frequency electric power generation with PZT ceramics. *IEEE-ASME Trans Mech* 2005;10:240–51.
- [10] Çevik G, Akşit MF, Şabanoviç A. Piezoelectric wind power harnessing – an overview. In: *10th int. Conf. on sustainable energy tech, Istanbul, Turkey*; 2011. p. 1–9.
- [11] Li S, Lipson H. Vertical-stalk flapping-leaf generator for parallel wind energy harvesting. In: *Proc of the ASME/AIAA conf on smart materials, adaptive structures and intelligent syst, California, USA*; 2009. p. 611–9.
- [12] Priya S, Chen C, Fye D, Zahnd J. Piezoelectric windmill: a novel solution to remote sensing. *Jpn J Appl Phys* 2005;44:L104–7.
- [13] Myers R, Vickers M, Kim H, Priya S. Small scale windmill. *Appl Phys Lett* 2007;90(5):54106.
- [14] Bryant M, Garcia E. Modeling and testing of a novel aeroelastic flutter energy harvester. *J Vib Acoust* 2011;133:011010.
- [15] Yun S-N, Ham Y-B, Park J-H. Energy harvester using PZT actuator with a cantilever. In: *ICCAS-SICE, Fukuoka, Japan*; 2009. p. 5514–7.
- [16] Lake J, Luan J, Tanaka Z, Liang B, Chen B. Piezoelectric materials and devices for wind energy harvesting. *Mater Res Soc Symp Proc* 2011;1325.
- [17] Fu H, Yeatman EM. A miniaturized piezoelectric turbine with self-regulation for increased air speed range. *Appl Phys Lett* 2015;107:243905.
- [18] Uchino K, Ishii T. Energy flow analysis in piezoelectric energy harvesting systems. *Ferroelectrics* 2010;400:305–20.
- [19] Renaud M, Fiorini P, Schaijk RV, Hoof CV. Harvesting energy from the motion of human limbs: the design and analysis of an impact-based piezoelectric generator. *Smart Mater Struct* 2009;18:035001.
- [20] Uzun Y, Kurt E. Performance exploration of an energy harvester near the varying magnetic field of an operating induction motor. *Energ Convers Manag* 2013;72:156–62.
- [21] Song Y, Yang CH, Hong SK, Hwang SJ, Kim JH, Choi JY, et al. Road energy harvester designed as a macro-power source using the piezoelectric effect. *J Hydrogen Energy* 2016;41:12563.
- [22] Friswella MI, Adhikari S. Sensor shape design for piezoelectric cantilever beams to harvest vibration energy. *J Appl Phys* 2010;108:014901.
- [23] Adhikari S, Friswell MI, Inman DJ. Piezoelectric energy harvesting from broadband random vibrations. *Smart Mater Struct* 2009;18:115005.
- [24] Uzun Y, Demirbas S, Kurt E. Implementation of a new contactless piezoelectric wind energy harvester to a wireless weather station. *Elektron Elektrotech* 2014;20:35–9.
- [25] D220-A4-103YB Datasheet [Accessed 29 October 2016], <http://www.piezo.com/catalog8.pdf%20files/Cat8.49.pdf>; 2011.
- [26] D220-A4-103YB Datasheet [Accessed 29 October 2016], <http://www.piezo.com/catalog8.pdf%20files/Cat8.50.pdf>; 2011.
- [27] Kurt E, Uzun Y, Durmuş C. Power characteristics of a new contactless piezoelectric harvester. In: *Int conf electric power and energy conversion syst, Sharjah, UAE*; 2015. p. 1–4.
- [28] Uzun Y, Kurt E. The effect of periodic magnetic force on a piezoelectric energy harvester. *Sens Actuator A-Phys* 2013;192:58–68.
- [29] Uzun Y, Kurt E, Kurt HH. Explorations of displacement and velocity nonlinearities and their effects to power of a magnetically-excited piezoelectric pendulum. *Sens Actuator A-Phys* 2015;224:119–30.